THESIS FOR THE DEGREE OF DOCTOR OF PHILOSOPHY

Power-generation, Power-electronics and Power-systems issues of Power Converters for Photovoltaic Applications

BJÖRN LINDGREN

Department of Electric Power Engineering
CHALMERS UNIVERSITY OF TECHNOLOGY
Göteborg, Sweden, December, 2002

Power-generation, Power-electronics and Power-systems issues of
Power Converters for Photovoltaic Applications
BJÖRN LINDGREN
ISBN 91-7291-216-2

© BJÖRN O. LINDGREN, 2002
Revision 1, December 2002

Doktorsavhandling vid Chalmers tekniska högskola
Ny serie nr 1898.
ISSN 0346-718X

Report number for the School of Electrical Engineering: 432

Department of Electric Power Engineering
Chalmers University of Technology
SE-412 96 Göteborg
Sweden
Telephone +46 (0)31-772 1000

Chalmers Bibliotek, Reproservice
Göteborg, 2002

Power-generation, Power-electronics and Power-systems issues of
Power Converters for Photovoltaic Applications

BJÖRN O. LINDGREN
Department of Electric Power Engineering
Chalmers University of Technology

Abstract

The thesis deals with issues related to solar energy systems, or more specifically, the electric systems of photovoltaic (PV) installations. Initially aspects of planning and estimating the performance of a PV-installation are considered. As the test site showed to have poor energy yield due to shading, a decentralised converter system was suggested for that and similar systems which result in a higher shading tolerance. The operation of single-phase inverters connected to the grid is investigated, especially the nature of hysteresis (bang-bang) controlled inverters and their interaction with the grid and other inverters. A novel switching method is suggested with similar features as of the hysteresis technique. The impact on harmonics on the grid from many inverters is investigated and showed to be decreasing with the increasing number of inverters.

The design and construction of a 110 W, single-phase PV-inverter is presented and discussed. The advantages and disadvantages of a common ac-bus compared with a common dc-bus are treated.

Voltage variations are discussed, for a low-voltage network with an extensive amount of photovoltaic generators or other types of embedded generation like fuel cells or microturbines. A number of analytic expressions are derived for the voltage profile of a feeder in these networks. Examples are given where the overvoltage on the grid due to active power injection is severe. *However*, allowing the inverters to inject or consume an amount of reactive power dependent on the local rms voltage is shown to eliminate this potential problem. A simple algorithm for this reactive power control is proposed and tested.

Keywords: Bang-bang control, Current control, Embedded generation, Photovoltaic, Power quality, Power systems, Shading tolerance, Solar power generation.

LIST OF PUBLICATIONS

This thesis is based on the work contained in the following papers:

Paper A

B. Lindgren, P. Carlsson and L. Cider
"Yield Losses due to Shading in a Building-integrated PV Installation; Evaluation, Simulation and Suggestions for Improvements", Published at the 2nd World Conference and Exhibition on Photovoltaic Solar Energy Conversion, Vienna 1998.

Paper B

B. Lindgren
"Topology for Decentralised Solar Energy Inverters with a Low Voltage AC-Bus", Published at the 8th European Conference on Power Electronics an Applications (EPE'99), Lausanne, Switzerland, 7-9 September 1999.

Paper C

B. Lindgren
" A PV-module Oriented Inverter, Feeding a Low Voltage AC Bus" Published at 16th European Photovoltaic Solar Energy Conference and Exhibition, Glasgow, May 2000.

Paper D

B. Lindgren
”A 110 W Inverter for Photovoltaic Applications”, Published in International Journal of Renewable Energy Engineering, April 2002.

Paper E (technical letter)

B. Lindgren, M. H. J. Bollen, O. Carlson
"Single-phase Current Control by Predefined Variable Switching Frequency" submitted to IEEE Power Engineering Letters.

Paper F

B. Lindgren, M. H. J. Bollen, O. Carlson
"Voltage Control of Low-voltage Feeders with Photovoltaic Generators" submitted to IEEE Transactions on Power Delivery.

Paper G

B. Lindgren, M. H. J. Bollen, O. Carlson
"Harmonics on the Grid from Single-phase Hysteresis Controlled Inverters " submitted to IEEE Transactions on Energy Conversion.

Paper H

M. H. J. Bollen, B. Lindgren, O. Carlson
"Voltage Drop Along a Feeder with a Large Number of Inverters Equipped with Voltage Control" submitted to IEEE Transactions on Energy Conversion.

Preface

The work involved in this thesis has been carried out at the department of Electric Power Engineering of Chalmers University of Technology.

I would like to thank Docent Ola Carlson who initiated this research project and has supported my work during the years. I would also like to thank my examiner Professor Mathias Bollen without whom this thesis not had been finished in the way it was (both in time and contents). During the years I have had good relations with Kjell Jonasson and Ingemar Andersson, representatives from the Research Foundation at Göteborg Energi AB which I appreciate. Docent Per Johander should also be thanked as an initiative force to this project. I would also like to thank my colleagues at the department for pleasant times.

Last but not least, I would like to thank my wife Viktoria and my sons, Aron and Frej who made life worth struggling during difficult times.

Acknowledgement

The Research Foundation at Göteborg Energi AB is gratefully acknowledged for its financial support.

A sub-project was financed by Elforsk, Swedish Electrical Utilities' Research and Development Company, which hereby is gratefully acknowledged.

The co-operation with IVF, Industrial Research and Development Corporation is also gratefully acknowledged.

Table of Contents

1. Introduction

The sun has a great potential to supply our society with large amount of energy with little impact on the environment. Governments around the world have signed agreements of reducing their emission of carbon dioxide while the need of energy is increasing. This has led to large programmes to support and subsidise investments in the photovoltaic (PV) area. The most extended are found in Japan, Germany and the USA. Japan has 450 MW_p (peak power) installed with a goal of 1100 MW_p in 2010 and for Germany the figures are 150 MW_p and 450 MW_p respectively. Another sign that PV are in progress is that oil companies (e.g. BP and Shell) are investing large amounts in PV-manufacturing plants and are among the largest PV-suppliers in the world.

In 1995, a demonstration photovoltaic power plant was inaugurated at Sankt Jörgen's Park in Göteborg, Sweden. It was funded by the Research Foundation of Göteborg Energi AB and was realised in co-operation with Göteborg University and Chalmers University of Technology. The plant is a base for building up knowledge in the photovoltaic area. At Sankt Jörgen, 48 photovoltaic modules each consisting of 72 cells and having an area of 0.9 m^2, are connected through an inverter to the public grid. Twelve PV-modules are connected to a DC/DC-converter feeding a 48 V battery system. All together the installed peak power is 6.6 kW.

In 1997, an evaluation of the power plant was performed. The result was discouraging due to shading and poor design. This is not a unique situation, see [1-3]. **Paper A** describes a method for simulating the expected energy production of a solar power plant and compares the expected production with the actual energy yield. It also discusses some of the mistakes made at Sankt Jörgen and suggests a number of measures that would improve the performance of the power plant.

One suggestion to improve the performance is to decentralise the power conversion [4-7], thus making the PV-plant more shading-tolerant. **Paper B** compares a number of possible configurations of PV-modules and inverter topologies and suggests a PV-module based inverter that would improve the energy yield of the power plant.

A PV-module inverter has been designed and constructed. In **Paper C** the implementation of hysteresis current control and the issue of a combined unipolar and bipolar voltage output modulation are discussed. Some simulations and measurements are also presented.

In **Paper D** the total design and performance is presented. The current controller has been implemented in an inexpensive 8-bit micro controller, with hysteresis control. The emphasis has been on high energy-efficiency and high power quality.

In **Paper E** (which is a technical letter) the implementation of a novel switching strategy is discussed which utilises the microcontroller in a better way than hysteresis control. The total harmonic distortion is decreased but the content of low-order harmonics in the output current becomes somewhat higher compared with the hysteresis control.

When PV-generation becomes common, there is a risk of overvoltages on feeders due to the injected active power. This in turn reduces the design margin for feeders and leads to more expensive distribution networks. **Paper F** shows some simulations of this phenomenon and suggests reactive power control for PV-inverters to minimise the voltage variation.

Harmonics on the grid from one and from several PV-inverters with hysteresis control is discussed in **Paper G**. Results from simulations and from measurements from Sankt Jörgen's Park are also presented.

A number of analytic expressions for the voltage profile of a feeder are derived in **Paper H**. This was done in Paper F for the discrete case and here the continuous case is treated.

2. Aim of the work and contribution

The aim of this project is to build up knowledge around PV-systems. The first part of the research concerns the optimisation of PV-installations, including energy yield estimation and system selection i.e. issues that are concerns for the users today. The contribution from this project concerns mainly power electronic issues as a suggested switching strategy and the combination of bipolar and unipolar switching of a single-phase inverter.

In the second part the research focused on power-system issues. These are not a problem today, as the energy delivered by PV-installations today is small compared with other sources and energy consumption. *However*, in the future, these issues will be a matter for the utilities and others to deal with. The contribution in this work is showing how voltage variation can be minimised in the low-voltage network by controlling the reactive power in every PV-inverter.

The application of the results obtained during this project is not limited to PV-installations only. Especially the power-system integration issues may also be applied to other inverter-connected sources like microturbines and fuelcells.

3. Power-generation

In Paper A, a method to investigate the production potential of PV-installations is described. The method considers the latitude and the horizon profile of the specific site to predict the amount of available energy. The difficult part concerns shading effects from objects close to the PV-panels that cannot be treated in the same way as 'horizon objects'.

At the time paper A was written (in 1997), available tools for simulation of PV-systems were investigated (Sundi, Radiance, PVsyst etc.) but none could perform a simulation regarding the electrical behaviour of the PV-cells including individual shading. A conventional simulation tool for electronics (P-spice, Simplorer, Saber etc.) would be far too slow if every PV-cell were to be simulated individually in a normal sized PV-installation. What is needed is an intelligent algorithm that sorts out which PV-cells are performing equally, depending on connection and shading. Then this algorithm could be added to the conventional tools without increasing the amount of calculations too much.

3.1 Photovoltaic cells

The photovoltaic effect is described in Encyclopaedia Britannica as “a process in which two dissimilar materials in close contact act as an electric cell when struck by light or other radiant energy”. In other words, a photovoltaic cell is a diode optimised to absorb photons from (usually) the sun and convert them into electrical energy.

Photovoltaic cells can be divided into four groups: crystalline cell, thin-film cell, dye-sensitised solar cell (DYSC or Grätzel-cell) and multilayer cell. The latter can also be considered as several layers of thin-film PV cells. The different types are described in [8] and [9]. The (mono- and multi-) crystalline are the dominating types with highest efficiency but the thin film cells are entering the market now. The thin-film technology has the potential to be manufactured at substantially lower cost than the crystalline cells. The production of PV-modules using thin-film technology can be fully automatised while for modules with crystalline cells, it is a bit of a handcraft.

In Figure 1 the electrical behaviour of a PV-cell is shown. Note that the current axis is in the other direction than for a normal diode.

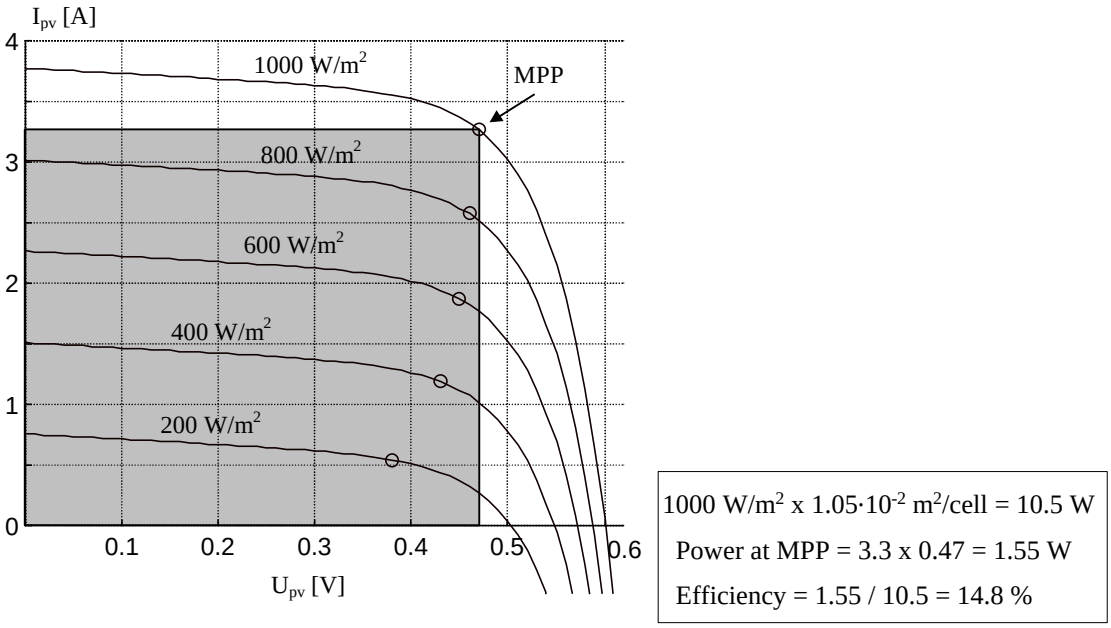

Figure 1, IV-curves for a PV-cell at different insolations.
Circles indicate the maximum power points.

At an irradiation of 1000 W/m^2, corresponding approximately to a cloud-free, sunny day, the upper curve shows that the open-circuit voltage of the cell is about 0.6 Volt. As the load (current) of the cell increases, the voltage decreases and at short-circuit (voltage = 0) the current is approx. 3.7 A for this particular cell (it depends on the size and efficiency). At open circuit and at short-circuit, no power is produced. At a point called the maximum power point (MPP), maximum power is gained from the PV-cell. To visualise this, a rectangle can be drawn from a point on the curve to the x- and y-axis. For the point where this rectangle has the largest area maximum power is generated.

At lower irradiation, the short-circuit current decreases approximately linearly with irradiation. The open circuit voltage does not decrease as much until very low irradiation. However, the open circuit voltage is much more affected by the temperature of the PV-cell. At a higher temperature, the open circuit voltage decreases. The phenomenon has quite a large impact and decreases the output power by approximately 15 % at a temperature increase from 25°C to 50°C.

3.2 Shading of Photovoltaic Installations

The striking conclusion when the measurements from the Sankt Jörgen's PV power plant were evaluated was the large impact shading has on energy production. The reason for this showed to be the way the PV-modules were connected in combination with their spatial formation.

To understand the shading of PV-cells in series, the second quadrant of the iv-curve and the reverse voltage break through, or the avalanche effect of a diode [10], must be considered. In Figure 2, the IV-curve for quadrants one and two is shown.

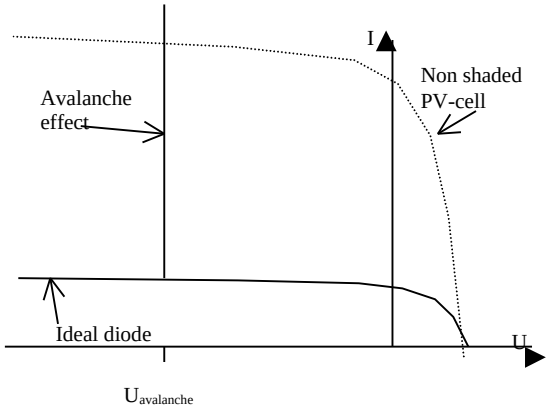

Figure 2, IV-curve of a 25 % illuminated PV-cell.

An ideal diode can withstand any reverse voltage and in the case of an ideal PV-cell it will work as a constant current load if reverse voltage is applied. In a series of PV-cells this means that the least illuminated cell will limit the current from the whole series. In reality, there is a point of break-through in the pn-junction when the externally applied electric field will overcome the intrinsic electric field, known as the avalanche effect. For a silicon PV-cell, this will happen at 14-30 V ($U_{avalanche}$). Subsequently, the maximum current through a series of PV-cells is no longer limited by the shaded cell, but the cell will dissipate power equal to the avalanche voltage times the current.

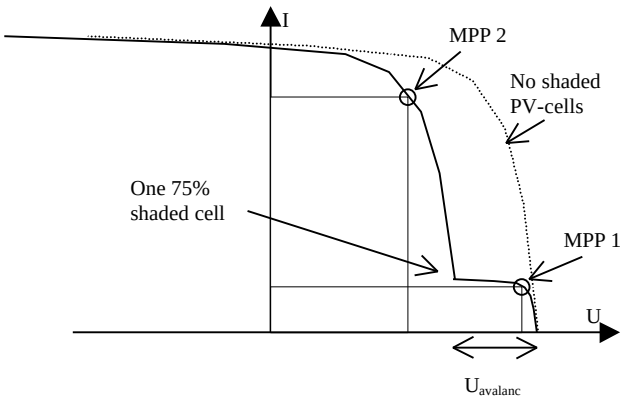

Figure 3, IV-curve of series connected PV-cells with different illumination.

Figure 3 shows the iv-curve of a series of three PV-cells, where one cell is shaded by 75 %. It can be noted that the curve now has two local maximum power points; MPP1 and MPP2. Which one is the global MPP, depends on how many cells there are in the series and on the $U_{avalanche}$.

At MPP 1, the voltage is not reversed for the shaded cell, and produces energy at its MPP, while all the non-shaded cells just produce approximately 25 % of their potential power. At MPP 2, the voltage of the shaded cell is reversed and the cell consumes energy. The rest of the cells produce more energy than in MPP 1, although not at their MPP. The somewhat paradoxical phenomenon occurs that the shaded cell heats up much more than the non-shaded cells. This could lead to damage to the shaded cells.

To avoid destruction of PV-cells due to this 'hot-spot effect', manufacturers connect by-pass diodes over a group of cells, for instance over 8 cells, see Figure 4. With this arrangement a substring with a shaded cell will be short-circuited by the by-pass diode and the non-shaded substrings can work at their MPP, but the energy from the by-passed substring is lost. It is important to underline that this is normally only a method for the protection of the PV-cells. If by-pass diodes are to be used to make the PV-module more shade-tolerant, they should be connected to significantly fewer PV-cells. Another method to gain shade tolerance is to install more power converters, as they will work independently of each other.

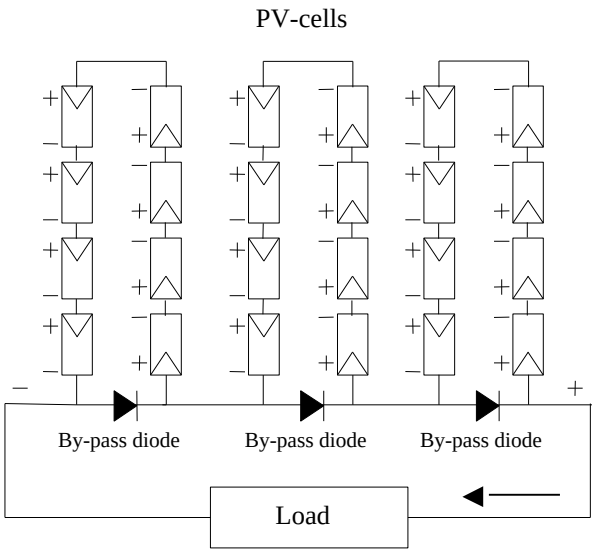

Figure 4, Three substrings by-passed with diodes.

3.3 Decentralised PV-inverters

The most effective measure to take in order to maximise the energy yield from a PV-installation is to place the solar panels in an optimal way. Having the right direction south/north (azimuth) and elevation angle can be evaluated in simulation programmes. It is also important to keep in mind that any shading of the solar panels will lead to considerable reduction in energy yield, even if just a small fraction of the panels is shaded.

Shading can rarely be completely avoided, certainly not in urban or suburban environments. At higher latitudes (like in Sweden) the sun is often close to the horizon which makes the shading problem more severe than at low latitudes. Therefore especially for high-latitude locations and urban/suburban sites, a shading-tolerant system should be chosen. That means: selecting more power converters with a low power rating and PV-panels with more by-pass diodes and avoid connecting PV-modules in parallel.

For the PV-installation at the Sankt Jörgen's Park, a decentralised power converter system was selected (Paper B) and realised (Paper C-D) with a 110 W inverter per module.

4. Power-electronics

4.1 Selection of system and converter

In Paper B, nine different converter systems for PV installations are investigated in terms of energy efficiency, cost, insulation and fault tolerance. One of the nine systems is the conventional way with one central inverter and the rest are of decentralised nature. The study is based on simplified assumptions of the fundamental function of the topologies, component losses and prices. In order to limit the extent of the work, detailed control issues are omitted. The conclusion of the study is that the centralised inverter is superior both in respect of efficiency and cost per watt. Among the decentralised systems, a solution with low voltage ac-bus is attractive. According to the calculations it has a higher efficiency and lower cost. This led to the choice of designing and building decentralised inverters for the PV-installation at Sankt Jörgen.

4.2 Inverter development

During this project, an inverter for photovoltaic modules has been developed. The design and function of the 110 W inverter are described in Paper C and Paper D and in the licentiate thesis [8]. The single-phase, full bridge inverter converts the 25-50 V dc from a PV-module to a 15 V, 50 Hz ac-voltage. The power is then transformed to grid level by a central transformer, see Figure 5.

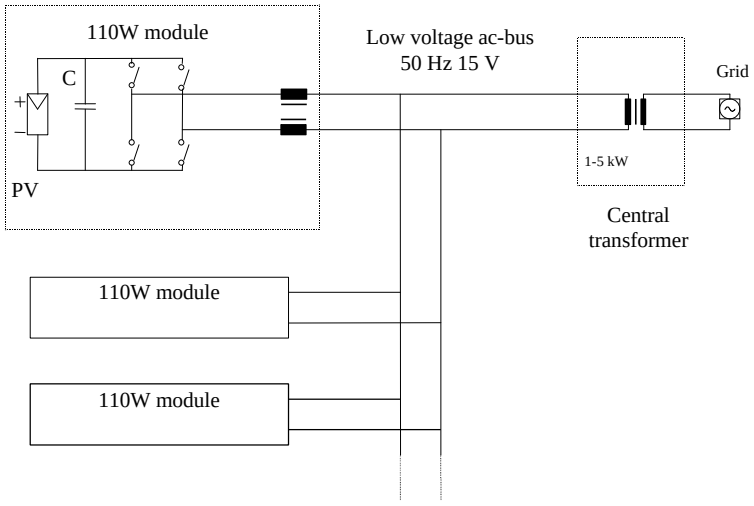

Figure 5, Decentralised PV-system with a low-voltage ac-bus.

The advantage of having a central transformer instead of one small transformer in each inverter is the higher efficiency of the larger transformer. The disadvantage is higher currents on the bus, which must be kept short to minimise losses in wires. Another disadvantage with a central transformer is that the PV modules are galvanicly in connection with each other. This may result in stray currents and/or earthing problems. However, the tested inverters have not shown any of these problems.

Knowing the size of a 110 W panel, the losses in wires can be estimated:

Current: 110 W / 15 V = 7.3 A
Solar panel size: 1.3 x 0.6 m
Interconnection copper wire: 2.5 mm^2 => 7.6e-3 Ω/m
Resistance per wire pair: 2 * 0.6 * 7.6e-3 = 9.12e-3 Ω
Power loss with 1 unit: 9.12e-3 * 7.3^2 = 0.5 W => 0.4 %
Power loss with n units in a row:

$$P_{wire} = \sum_{i=1}^{n} RI_i^2 = \sum_{i=1}^{n} R \cdot (iI)^2 = RI^2 \frac{n(n+1)(2n+1)}{6} \qquad (1)$$

Now, consider ten solar panels in a row with a 1.1 kW transformer in the middle as in Figure 6. That makes two symmetrical busses with five modules in each direction:

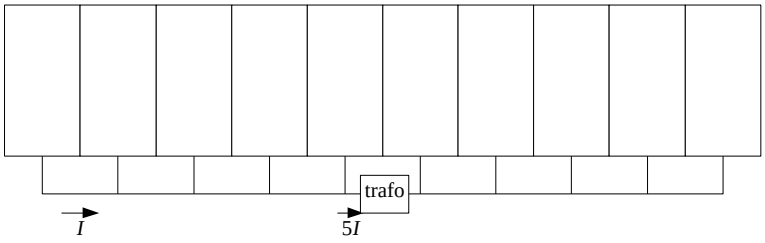

Figure 6, Ten solar panels with wiring and a common transformer.

Relative loss: $\frac{RI^2 5(5+1)(2 \cdot 5+1)/6}{5 \cdot 110} = 0.05$ => 5 % (2)

This loss is at rated power but only some 20 % of the solar energy is captured at full power. The following weight function is referred too as the 'euro sun distribution':

$$h = 0.03h_5 + 0.06h_{10} + 0.13h_{20} + 0.10h_{30} + 0.48h_{50} + 0.20h_{100} \qquad (3)$$

with η the average power, η_5 the power at 5 % insolation, etc. Combining (2) and (3) gives an average wire loss of 2.4 %. Due to the maximum current of 5 x 7.3 = 36 A closest to the transformer a cable of 4 or even 6 mm^2 is more appropriate and will reduce the wire loss further to 1.5 % or 1 % respectively.

4.2.1 Three generations of the 110 W PV-inverter

The design process took several iterations to accomplish. The first prototype, see Figure 7, was of conventional PWM-type with a fixed switching frequency.

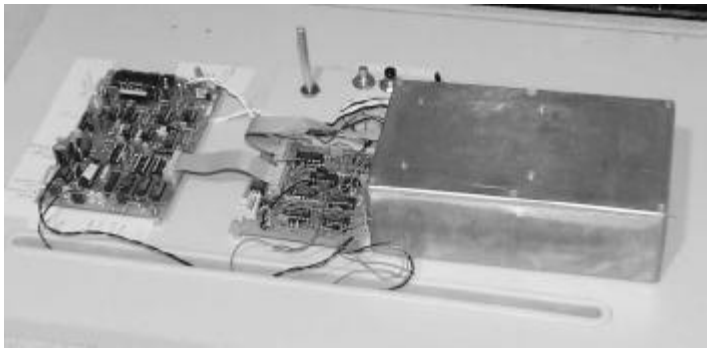

Figure 7, First prototype of the 110 W inverter.

An analogue P-controller shaped the grid current proportional to the grid voltage using double pulse modulation. The advantage with this technique is that a high switching frequency can be achieved and that the switching frequency is easy to change. Drawbacks are noise sensitive analogue circuitry, it need to be tuned and it takes a lot of discrete components to realise.

Problems with interfering signals which is common on switched power converters and the desire of a more flexible platform took the project to a digital design, see Figure 8.

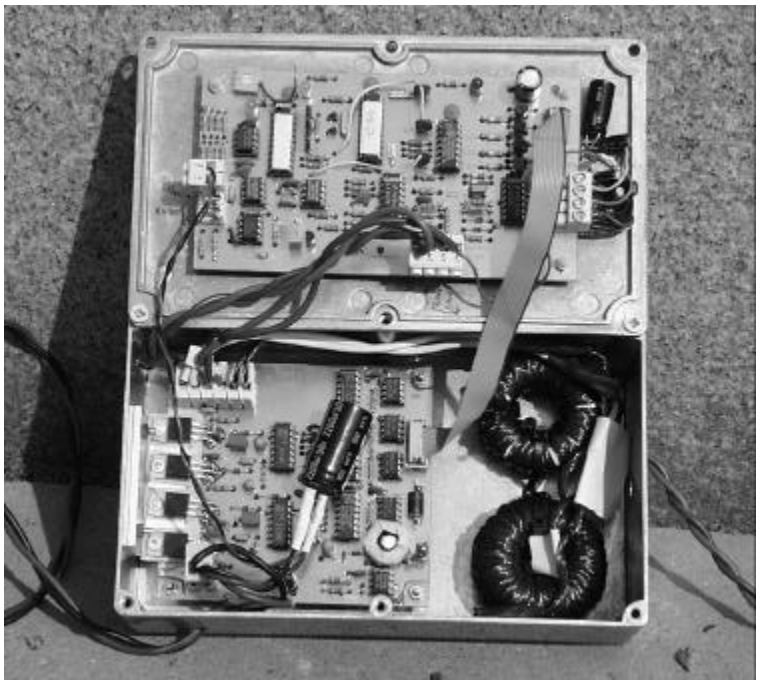

Figure 8, Second prototype of the 110 W inverter.

The inverter with a micro controller as current controller was divided into two separate circuit boards. On top: the controller card with two micro controllers (Atmel: AT90S2313), analogue to digital converters and protection circuits. In the bottom the main circuit with the four MOSFET:s, dc-capacitor, grid inductors and the transistor driving circuitry is seen.

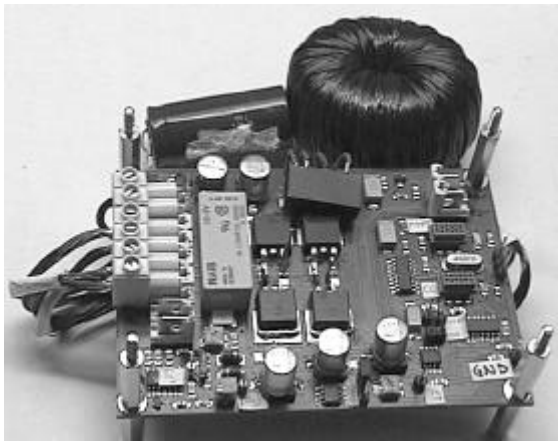

Figure 9, Third prototype of the 110 W inverter.

The third generation is a complete PV-inverter design on a double sided, surface mounted circuit board (70 x 100 mm), see Figure 9. The dc capacitor and the line inductor are not mounted on the PCB due to their size. The inverter contains all necessary functions as sleep and wake-up

function (to be completely switched off during the night), grid voltage supervision circuit, a relay to disconnect the inverter at abnormal conditions and a communication interface (RS485).

4.2.2 Function

The PV-inverter consists of a single-phase full bridge with an input (dc) capacitor of 1.4 p.u. (2200 μF) and a line filter of 0.15 p.u. or 980 μH (p.u. is in respect to rated voltage, power and fundamental frequency). Four MOSFET-transistors are employed as switches. The block scheme is seen in Figure 10.

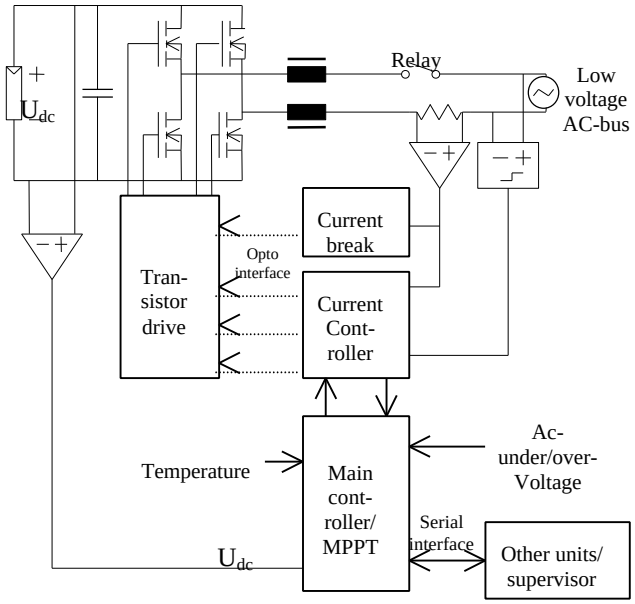

Figure 10, Block diagram of the 110 W inverter.

The current controller has an internal sinusoidal reference generator (look-up table) which is synchronised with the grid voltage. The grid current is measured over a shunt resistor and is fed to the current controller and to overcurrent protection circuitry. The main controller performs maximum power point tracking and general supervision as grid voltage monitoring, start up and sleep-condition testing etc.

4.3 Dc-bus versus ac-bus

In paper B a study is presented in which different converter configurations were compared. The conclusion from this paper was that several configurations performed similar in respect of system efficiency. One topology with low-voltage ac-bus was selected based on this study (as described above). During the design and evaluating of the inverter, certain aspects came up that were not included in the study. For instance the difference in complexity of controlling an inverter and a dcdc-converter. Therefore a study of dcdc-converters was accomplished one and a half years later.

4.3.1 Prerequisites

The prerequisite was that the shade tolerant system should remain. Therefore the ac-bus was exchanged by a dc-bus and the inverters by dcdc-converters with a rated power of 110 W (the same as for the inverters). The dcdc-converters are feeding the dc-bus from each solar panel, see Figure 11.

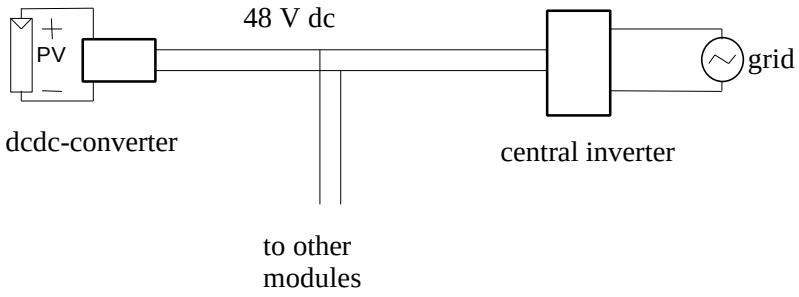

Figure 11, System configuration with 48 V dc-bus.

In this system, a central inverter has to transfer the power from the dc-bus to the grid, controlling the voltage of the dc-bus. The bus voltage was selected to 48 V because boost converters were to be used (which can only increase the voltage from the PV-modules of 25-45 V) and a higher bus voltage would make the comparison with the ac-bus difficult. An advantage of this system would be that voltage control of the grid voltage (see Paper F and Paper H) becomes easier. Only the central converter needs a controller. Voltage drop in the dc 48-Volt system is less of a problem compared with 15 Vac.

4.3.2 Two prototypes of dcdc-converters

Two dcdc-converters were studied; one single-phase boost converter and one 4-phase boost converter, see Figure 12.

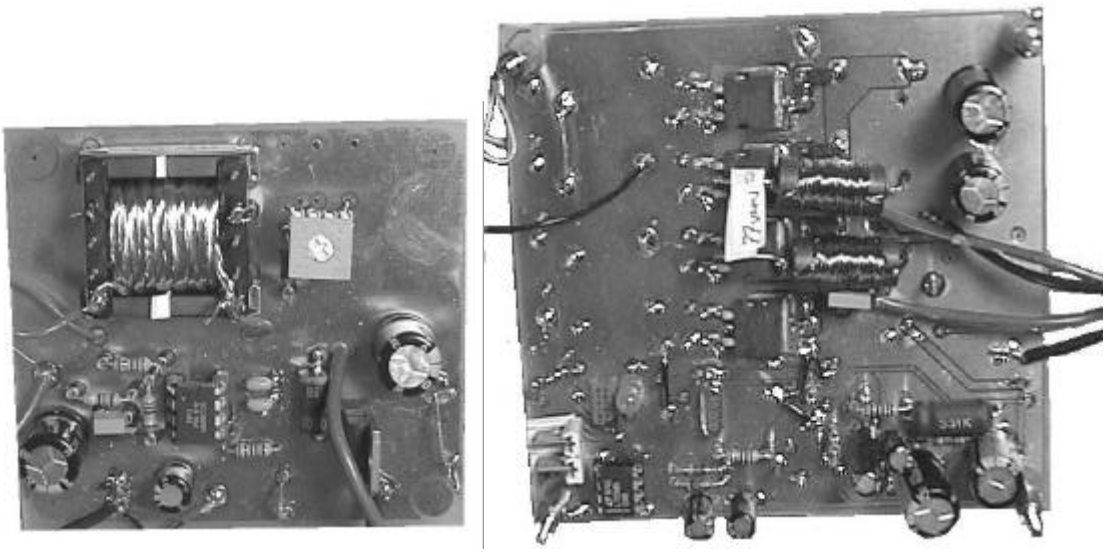

Figure 12, One phase- and four-phase boost (dcdc) converters.

The reason for making the 4-phase boost converter was to compare efficiency and inductor size if the energy is converted through four small parallel stages instead of one.

The dc-converters can be operated in two ways. Either with a fix duty cycle (‘dc-transformer’) or individually controlled. In order to maintain a shading tolerant system, each dcdc-converter performs the maximum power point tracking (MPPT) to load their PV-module optimally

4.3.3 Conclusions

The conclusions from this study were that the 4-phase boost converter had somewhat higher efficiency at full power but inferior over-all performance, mainly due to the power consumption of the additional drive circuits. The efficiency for a dcdc-converter compared with the inverter was approximately 95 % instead of 90 % in the power range 0.3-1.0 p.u. and superior in the low power range. In Figure 13 the system efficiency is shown when a central inverter (for the dc-system) and a transformer (for the ac-system) is included respectively.

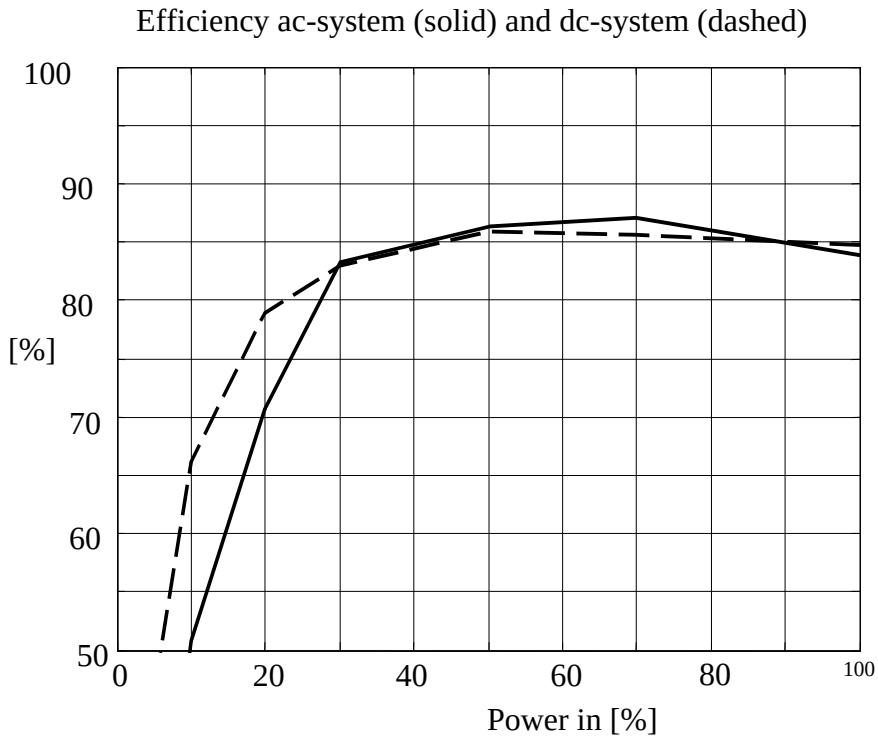

Figure 13, Efficiency comparison between systems with ac- and dc-bus.

Additional to this advantage of higher efficiency for the dcdc-converter, the maximum power point tracking is easier to achieve. This is because a single-phase inverter has a pulsating power delivery, while the optimum for a photovoltaic source is a constant power flow (at the MPP). The dc-capacitor has to buffer the difference. In the case a small capacitor is selected, the operating point in the PV's IV-curve will oscillate considerably and can easily go towards too low input voltage. In the case the dc-capacitor is made extremely large, the MPP will be hard to track due to the slow response in voltage change - and the inverter becomes expensive. (The problem with pulsating power flow can be avoided by using 3-phase inverters but this will increase the cost even further.)

The cost at low volume production is also in favour for the dcdc-converter. Even though the central inverter needed is far more expensive than the central transformer, the total cost for the dc-system is lower, according to calculations made for systems made of standard components and at low production volumes (1000 power converters). Though, at larger volumes, this difference might become smaller, as special designed integrated circuits (ASICs) can be beneficial which reduces the number of integrated circuits.

A disadvantage with the dc-system is lower reliability due to the central inverter, which has shorter mean time between failure than the central transformer.

4.4 Variable Switching Frequency

In the technical letter, referred to as Paper E a novel switching method is presented. It is based on the same principal as the hysteresis control, namely predefined ripple amplitude in the output current. The switching frequency will vary and be lower at the peak voltage and current (at high power factors) compared with fixed switching frequency with the same average switching frequency. This leads to lower switching losses, as they are proportional to instantaneous value of the current and the number of switching transitions. To minimise the *THD* of the output current the ripple amplitude should be constant throughout the period of the fundamental frequency. This method allows for designing the ripple amplitude arbitrary, hence the switching losses can be decreased further at the expense of a higher THD_i. This is also possible for the hysteresis control *but* in a digital implementation the microcontroller is utilised in a better way so the average switching frequency could be increased. Another advantage of the proposed switching algorithm is that the minimum and maximum switching frequencies are known (so is the distribution) when the design calculations are made. Therefore the method is referred to as Predefined Variable Switching Frequency (PVSF).

4.4.1 Calculations

In order to calculate the required switching period throughout the fundamental cycle, the inductance equation (left hand equality of (4)) is used. From Figure 14 the voltage over the inductor is given (right hand equality of (4)).

$$u_L = L\frac{di_g}{dt} = u_{H-bridge}\left(U_{dc}, switching\_state\right) - u_{grid}(t) \qquad (4)$$

where *switching_state* is either -1, 0 or 1.

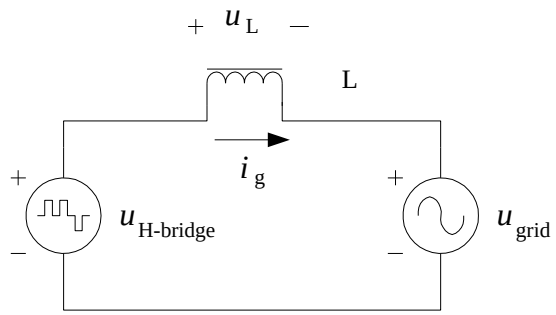

Figure 14, Basic scheme of the main circuit.

The explicit calculation code is given in Appendix B (Matlab code). The desired ripple could either be constant or varying sinusoidal. In Figure 15 the calculated switching period (solid) is shown with a constant ripple, U_g = 15 V, U_{dc} = 34 V, L = 1 mH, t_1 = 1 ms and t_2 = 7.5 ms. t_1 and t_2 are the instants where the output voltage changes between bipolar and unipolar mode (see section 5.3). For these values, the constant value of the ripple was chosen such that the minimum switching period (54 µs in Figure 15) is long enough for the controller to accomplish the calculations. This was done in order to minimise the current ripple.

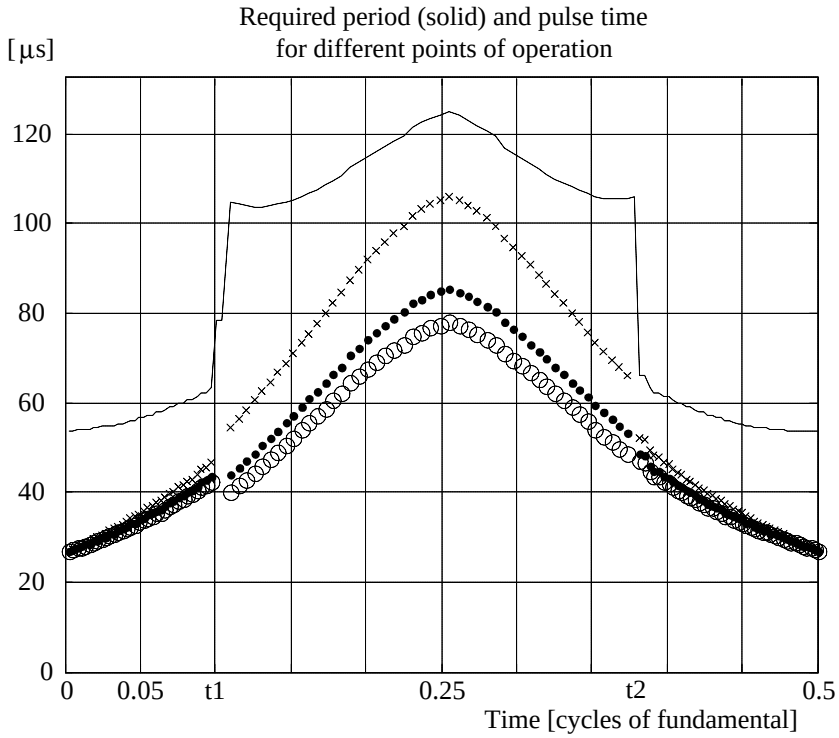

Figure 15, Pre-calculated switching period (solid) and required pulse time for three different points of operation during half a fundamental's cycle.

The three additional curves shown in Figure 15 give the required pulse time for different points of operation in respect of the dc (photovoltaic) source. Circles show the required pulse time for dc-values at the MPP at full insolation, dots at half insolation and crosses at half the nominal voltage and full current (not a MPP). These variations are one of the reasons why the pulse times cannot be implemented as a look-up table in the same way as the switching period is meant to be. The other reason is that the average level of the current must be controlled, as the slightest asymmetry would cause the current to drift.

4.4.2 Measurements

In Figure 16 a measurement of the output current is shown for the PVSF-method and in Figure 17 for a hysteresis-method (on the same hardware).

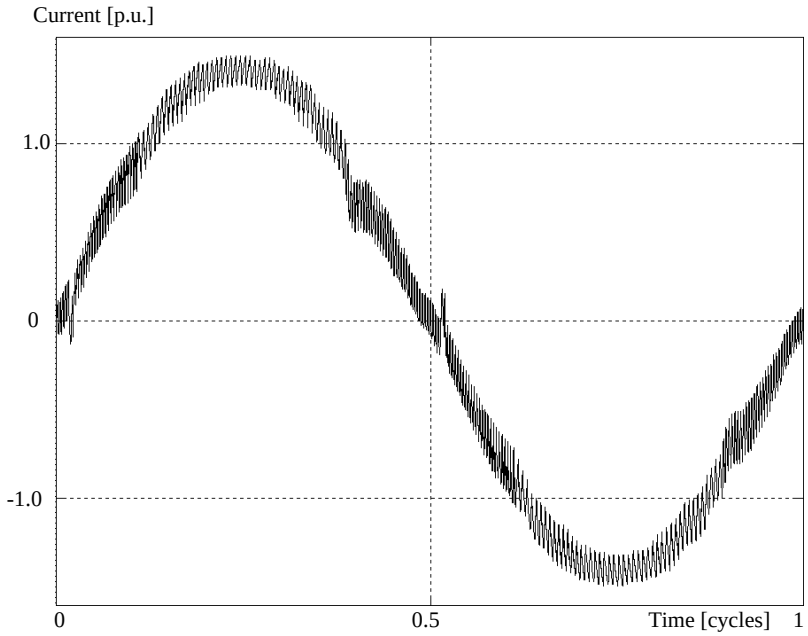

Figure 16, Output current with PVSF-control.

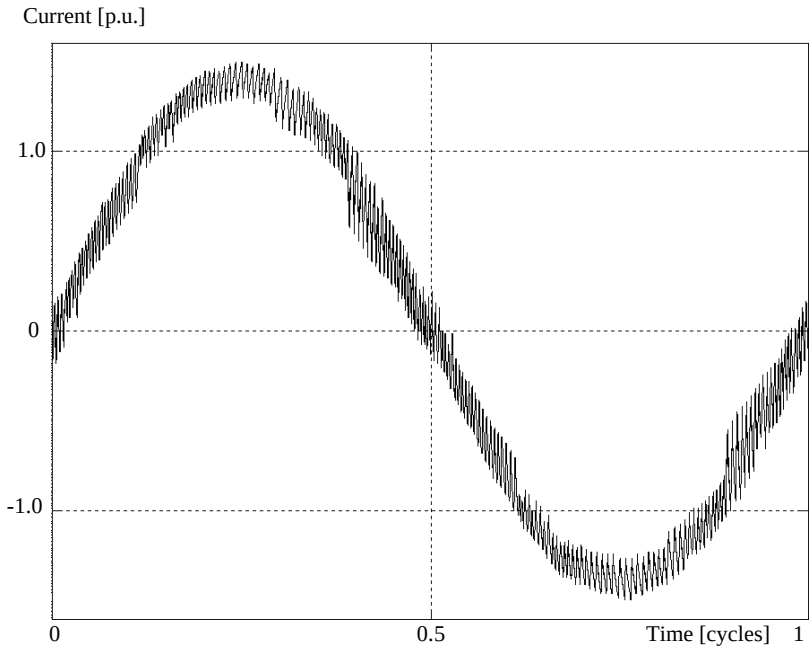

Figure 17, Output current with bang-bang control.

The average switching frequency for PVSF is measured to 11.5 kHz while the highest achievable switching frequency for the hysteresis controller was 10 kHz. This leads to a lower *THD* of the current of approximately 0.5 %-unit, shown in Figure 18

.

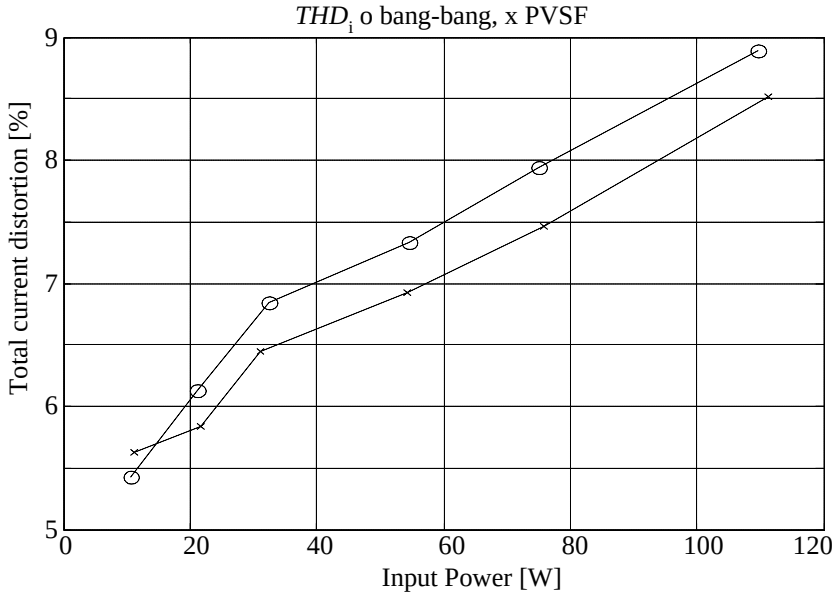

Figure 18, THD at varying power for bang-bang (o) and PVSF (x).

Drawbacks of this PVSF-method are that it depends on some quantities implying the need of tuning and it is difficult to implement a linear control-method for such a strongly non-linear system. For the measurements in Figure 16 and Figure 17 the latter can be expressed as a less sinusoidal shaped current. In Figure 19 the distortion of harmonics two to forty are shown as a function of power.

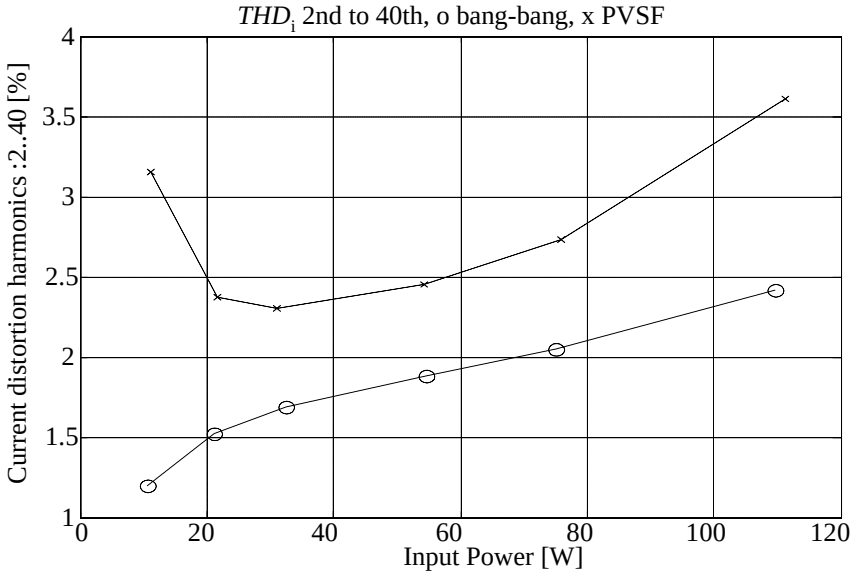

Figure 19, Distortion 2nd-40th harmonics, disregarding switching for bang-bang (o) and PVSF (x).

Here the current distortion from the PVSF-control is approximately 0.5 %-units higher than from the hysteresis control. Note however that the level is well below 10 % which is significantly lower than the distortion of standard low-voltage equipment like computers, customer electronics and fluorescent lighting. In Figure 20 the high frequency-content of the current (the difference between Figure 18 and Figure 19) is shown and the reduction is clearly seen for the PVSF method. The conclusion is that even if the wave-shape is worse (but not bad) the more severe high-frequency distortion is decreased.

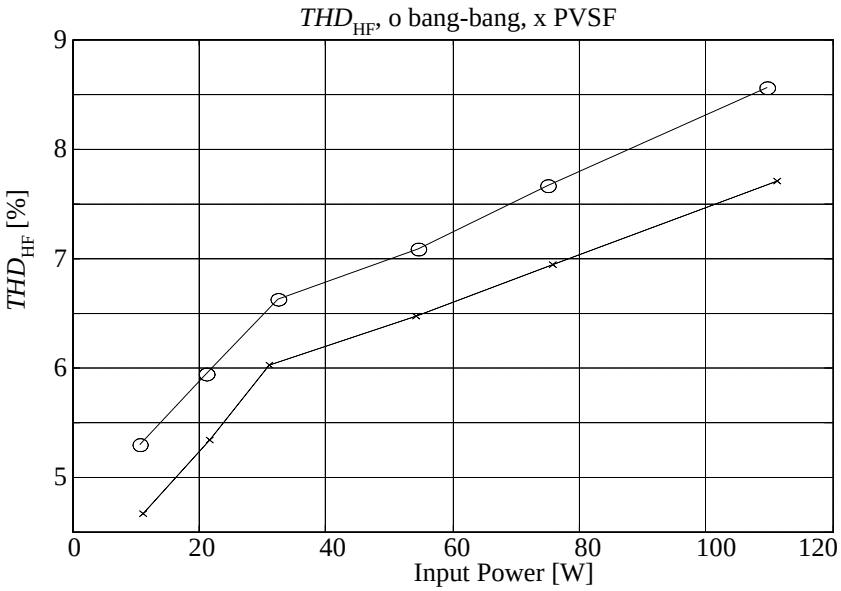

Figure 20, The high-frequency distortion from 41st harmonic and upwards.

5. Power-system issues

So far, the installed capacity of solar generated power is small compared with other production units and compared with the local power consumption and therefore power quality issues have not been an urgent matter. Issues around connecting solar panels to the grid have so far been a matter of energy yield optimisation, safety, reliability and cost.

In the first section the IEEE standard 929-2000, which addresses PV-to-grid connection, is summarised and commented.

5.1 IEEE Recommended Practice for Utility Interface of Photovoltaic Systems (IEEE Std 929-2000)

The standard (IEEE Std 929-2000) generally describes PV-systems, terminology and specially defines the circumstances, under which the PV-inverters should ‘disconnect’. The standard uses a longer term: “cease to energize the utility line” to allow the inverters to monitor the grid voltage while ‘disconnected’. The power-quality issues involved in this standard are: voltage fluctuations leading to flicker and distortion.

For smaller power plants, defined as total power less than 10 kW, the PV-inverter should trip if the grid voltage is outside the normal operation range (in the US it is 88-110 % of 120 V). The maximum time for the inverter to trip is specified for two ranges: if the voltage is outside 50-150 % of the nominal level, the device should trip in 0.1 seconds, else in 2.0 seconds (6 / 120 cycles). For larger systems, it is up to the utility to decide whether to trip at these levels or at others. The reason for this is that the utility might see the PV-plant as a power source, which increases the probability to ride through a disturbance on the grid.

A short paragraph concerning voltage fluctuations (flicker) expresses that PV-inverters connected to the grid should not result in larger voltage harmonics than stated in standard: IEEE 519-1992. Flicker, which is repeated voltage variations in the range 8-32 Hz, should not normally occur in a PV-plant. The only reasons for such variations should either be varying shading from rotating objects (wind turbines) or instabilities in the controllers of the PV-inverters. Never the less, the customer with PV is treated in the same way as any other customer and is therefore responsible for the emergence of flicker problems.

According to the standard the PV-inverter should monitor the grid frequency and disconnect at certain local levels (< 59.3 or > 60.5 Hz in the US). Considerably larger frequency ranges are also mentioned for cases where the variation naturally is larger, for example for small islands.

Islanding protection is discussed, and a very tough test procedure of this feature is described in the standard 929. It is important to note that this feature is optional. The manufacturer should state if his device has the "nonislanding feature" or not. If it has, the inverter should be able to disconnect if the grid is lost. A test set-up is described where the inverter has a perfectly matching load (both active and reactive) and the load has a resonance circuit with the quality factor of 2.5 (handles power 2.5 times the active power) and the frequency identical to the grid frequency. This is in theory impossible, because no current will go through the circuit breaker and it is therefore infeasible to determine if the circuit breaker is opened or closed. In practice however there are ways to solve this problem. Besides, in reality the perfect match and a resonance circuit of exactly 50/60 Hz is unlikely, but still the inverter has to pass this test.

5.2 Voltage issues

In the low-voltage network no production units are normally present. When solar generators are becoming more common, new phenomena might therefore arise. In Paper F and Paper H theoretical analysis is presented for voltages along a feeder equipped with solar generators. These theories are exemplified in Paper F by a number of simulations. The general conclusion is that if the PV-inverters inject pure active power, which is normally the case today, the voltage will vary in a considerably larger range than now. This would lead to that the utilities have to re-dimension their low-voltage network and install more transformers. *However*, if the PV-inverters are allowed to control the voltage at their connection point by producing or consuming reactive power, the voltage variation can be kept at the same magnitude as at present. The disadvantage of this control method is that the inverter has to be designed for a larger current than in the pure active-power case.

5.2.1 A Feeder with a discrete number of equally distributed equal loads

In Paper F, expressions for voltage variation is derived from the following general assumption, see Figure 21. A feeder is loaded with the same active (P_0) and reactive (Q_0) load at a number of nodes. The distance between

every node is the same so the impedance between two neighbouring nodes is $Z = R+jX$.

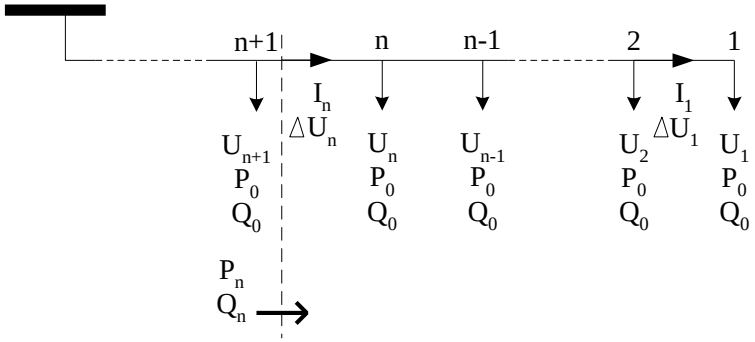

Figure 21, Scheme of a uniformly loaded feeder.

For a case with embedded generation (e.g. PV-panels) situations can arise when all nodes are net producing active power (a sunny summer day); $P_0 = -P_{pv}$. Normally, these inverters have a unity power factor so $Q_0 = 0$. This leads to a voltage difference between two nodes of:

$$\Delta U_n = -\frac{R}{U_0} P_{pv} n + \frac{n(n+1)(2n+1)}{6} \cdot \frac{Z^2}{U_0^3} P_{pv}^2 \qquad (5)$$

Where U_0 is the voltage at the substation (or the nominal voltage). The interesting with (5) is that the two terms have different signs. The first term represents a voltage increase due to active power injection and the second term is the voltage drop due to active and reactive power losses in the feeder's impedance. The first term usually dominates but at some distance (n) and at some power injection rate (P_{pv}) the voltage increase can be balanced. This is due to the second term has a higher power of n and P_{pv} (for real numbers this can be exemplified when X is dominating Z as for an O/H line). In the simulated example from Paper F (Figure 22) the voltage at the last node of a feeder is shown for varying active power injection (P_{pv}).

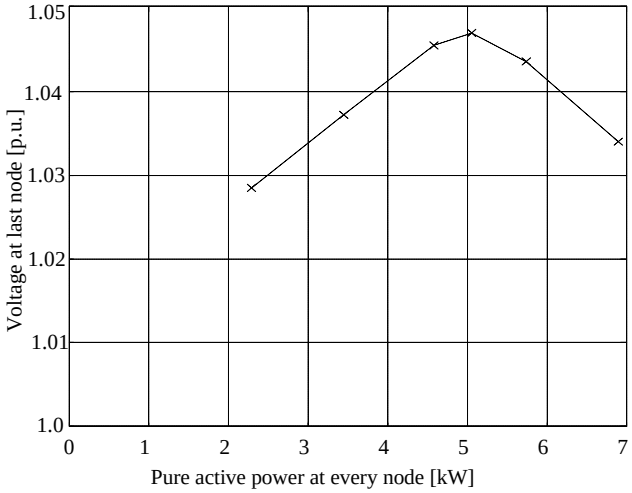

Figure 22, Voltage in the end of a feeder at different injection rates.

The worst case is if the production at every node is 5 kW. If the power is increased further, the overvoltage becomes lower. This can be explained from (5) as the voltage increase is proportional to the injected power whereas the voltage decrease is proportional to the square of the injected power.

5.2.2 A Feeder with equally distributed continuous load

In Paper H, expressions are derived for a feeder with continuous load. Including the feeder impedance is unfortunately shown to lead to non-linear differential equations which cannot be (or are difficult to) solve analytically. However, in order to understand voltage profiles we can neglect the feeder losses and solve the second order linear differential equations which results. Making the same assumptions as in the previous section (injection of pure active power) leads to the voltage profile:

$$U(s) = U_0 + \frac{rp_{pv}}{U_0}\frac{\left(L^2 - s^2\right)}{2} \qquad (6)$$

Where

U_0 is the voltage at the substation (or the nominal voltage)
r+jx is the feeder's impedance per unit length
p_{pv} is the injected active power per unit length
s is the distance from the end of the feeder towards the substation
L is the total feeder length

If the inverters are allowed to control the reactive power, the voltage variation can be decreased thus limiting over- and undervoltages. The

reactive power is controlled independently of the active power, and is proposed to depend linearly on the difference between the terminal voltage of the inverter and the nominal voltage (α is a constant):

$$q(s) = a\left(U(s) - U_0\right) \tag{7}$$

With this assumption the voltage profile becomes:

$$U(s) = U_0 + \frac{rp_{pv}}{ax}\left\{1 - \frac{\cosh\left(s\sqrt{ax/U_0}\right)}{\cosh\left(L\sqrt{ax/U_0}\right)}\right\} \tag{8}$$

The interesting thing with (8) compared with (6) is that the voltage rise is limited even for an infinite feeder length. Combining (7) and (8) in order to find the maximum reactive power needed (when s = 0 and L $\rightarrow \infty$) gives an expression independent of the value of a:

$$q_{\max} = \frac{rp_{pv}}{x} \tag{9}$$

The minimum power factor is only determined by the x/r-ratio of the feeder impedance. The maximum inverter current is thus:

$$I_{\max} = \frac{p_{pv} \cdot \Delta s}{U_0}\sqrt{1 + \left(\frac{r}{x}\right)^2} \tag{10}$$

The second factor in (10) gives the increase in current rating due to the controller. A feeder with a higher resistance will give a higher inverter current, because more reactive-power is needed to compensate for the voltage rise due to the active-power injection.

Expression (9) can be understood when realising that the control algorithm results in a flat voltage profile along the feeder, thus there is no longer any voltage drop:

$$-rp_{pv} + xq = 0 \tag{11}$$

5.3 Harmonic issues

In Paper G, aspects of harmonic distortion are discussed for PV-inverters connected to the grid. Parameters in the implemented hysteresis control are varied in order to investigate their impact on the grid current. Also the grid's impact on the inverter current control algorithm is studied.

The feasibility of using a combination of unipolar and bipolar output voltage is investigated. In Figure 23 the grid voltage and the switched output voltage are shown in the upper half.

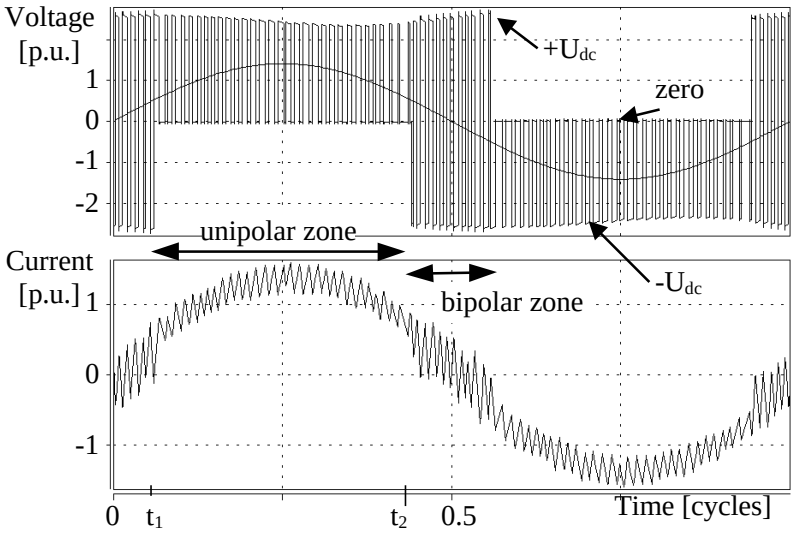

Figure 23, H-bridge voltage and grid voltage (top) and grid current (bottom).

The resulting grid current is seen in the lower half of Figure 23. In the standard double pulse modulation, the unipolar zone equals half the fundamental cycle (t_1=0 and t_2=0.5). The result of varying t_1 and t_2 is that the high frequency distortion decreases with increasing unipolar zone wile the odd low frequency harmonics have their lowest value when only using bipolar switching (unipolar zone equals zero). The odd low frequency harmonics increase with increasing unipolar zone but there is a local minimum approximately at t_1=0.05 p.u. and t_2=0.45 p.u. (as in Figure 23) which might be the optimal choice.

The general conclusion when several inverters are studied is that the relative high frequency content decreases with the number of units.

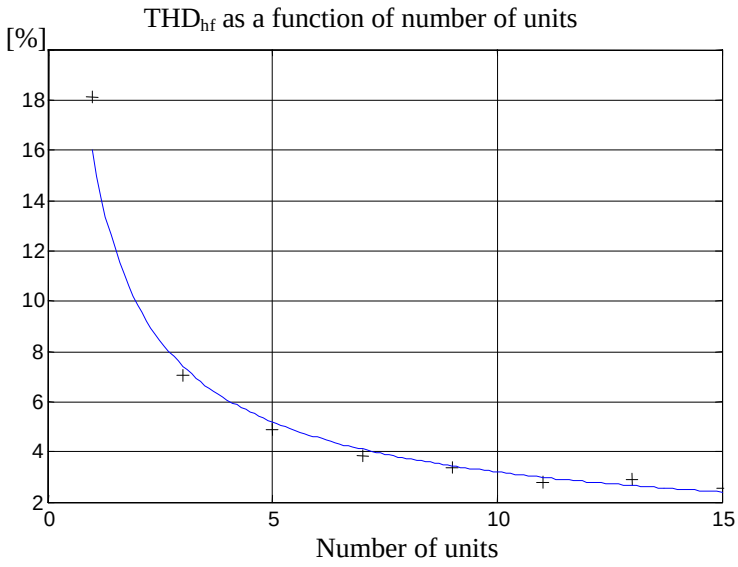

Figure 24, High-frequency current distortion versus number of inverters.

In Figure 24 the relative high frequency distortion is shown from simulations with one to fifteen inverters. The reason for this attenuation (or cancellation) is that even if the magnitude of the high frequency spectrum is similar for the units, the phase angles are not. In theory the curve in Figure 24 should be proportional to one over the square root of number of units if phase angles are totally random.

6. Conclusions

Shading effects on photovoltaic installations are discussed in this thesis and the general conclusion is that shading can have a very large impact on the energy yield. This means that precautions must be taken when a photovoltaic power source is planned, so the investment is not wasted. A method to analyse shading is offered, which estimates the loss due to shading of close objects.

One solution to solve shading problems is to choose a more decentralised converter system. Every subsystem then works independently of the others and makes the system more shade tolerant. A decentralised system can be achieved in several ways. The main issue is the selection of ac- or dc-bus. Using an ac-bus gives a truly modular and more fault-tolerant system while a system with dc-bus has higher efficiency and is less expensive.

The possibility of operating a single-phase full-bridge inverter in a combined unipolar and bipolar mode is discussed and realised. The advantages over conventional techniques are: another degree of freedom in order to optimise harmonic distortion and efficiency and an increased controllability compared with double pulse modulation or lower distortion compared with bipolar switching.

A novel switching method, called Predefined Variable Switching Frequency is presented (it also uses the combined unipolar and bipolar voltage output mode). It has similar features as the hysteresis technique namely the pre-definition of the ripple amplitude. This results for both techniques in a varying switching frequency. While the switching frequency variation is random for the hysteresis technique, the maximum, minimum and distribution of the switching frequencies are know for the proposed method. This is an advantage when designing filters and emc-design. The drawback is the resulting strongly non-linear control that requires careful tuning.

Embedded generation in the low-voltage network is discussed. The risk for overvoltage when injecting large amounts of active power to the low-voltage network is analysed. The harmonic distortion of the current injected by the inverter is also discussed. This discussion holds not only for photovoltaics but also for other inverter-connected sources like microturbines and fuel cells. A case study shows that with a fairly extended portion of PV-generated power, the feeders must be shortened to not violate the maximum voltage variations. This situation can be improved by

controlling the reactive power in the inverters and thereby decrease the voltage variation. A linear relation between the voltage deviation and the reactive power from/to the PV-inverter is proposed. With this control it is shown that the voltage on the feeder in the case study does not exceed the normal values and does not need to be re-dimensioned. It is shown by simulations and measurements that the harmonic distortion due to the inverter remains within acceptable levels.

7. Future Work

The simulation programmes used to estimate the energy yield from planned photovoltaic installations would benefit from the possibility to include shading from close objects. For this purpose the standard one- or two-diode models are not advisable due to their high computational demand. Some ‘intelligent’ algorithm to describe the energy production as a function of PV-cell interconnection and shading geometry is desirable.

The control of the PVSF-technique should be developed further. Especially the transition between unipolar output and bipolar output should be possible to improve as no ‘surprises’ in the wave-shapes are expected. Either tabulated adjustments of the linear-control could be applied or changing from the linear PD-control to some other technique, for instance fuzzy control. The controller needs not to have a good step-response but utilise that the system is well known as sinusoidal grid voltage, IV-curve of the photovoltaic cell, capacitor and inductor sizes.

The overvoltage on the low-voltage network has only been exemplified by case studies in this work. More comprehensive work is needed to estimate voltage variation generally. The goal should be guidelines for network design with embedded generation. Also rules should be developed to determine the value of the parameter α in the proposed reactive power control algorithm.

New research should also address how to handle islanding in the presence of distributed voltage control.

8. References

[1] C. Reise, A. Kovach. “PV Shading Analysis in Complex Building Geometries”, Proceedings of the 13th European Photovoltaic Solar Energy Conference, Nice, 1995, pp. 575-579.

[2] A. Reinders et. al. “2250 PV-Roofs in Germany – Operating Results from Intensified Monitoring and Analysis through Numerical Modelling”, Proceedings of the 13th European Photovoltaic Solar Energy Conference, Nice, 1995, pp. 575-579.

[3] V. Quaschning and R. Hanitsch “Shading of Integrated Photovoltaic Systems in Buildings”, 4th European Conference SolarEnergy in Architecture and Urban Planing, Berlin, 26-29 March 1996.

[4] H. Oldenkamp, I. De Jong, “Next Generation of AC-module Inverters ”, Proceedings of the 2nd World Conference on Photovoltaic Solar Energy Conversion, Vienna, 1998, pp. 2078-2081.

[5] D. Schekulin et.al. “Module-integratable Inverters in the Power-range of 100-400 Watts”, Proceedings of the 13th European Photovoltaic Solar Energy Conference, Nice, 1995, pp. 1893-1896.

[6] M. Shafiyi, A. Louche “AC-modules for Autonomous and Grid Connected Applications”, Proceedings of the 13th European Photovoltaic Solar Energy Conference, Nice, 1995, pp. 1906-1909.

[7] W. Knaupp et.al. “Operation of a 10 kW Façade with 100 W AC Photovoltaic Modules”, 25th IEEE Photovoltaic Specialists Conference, Washington DC, 1996.

[8] B. Lindgren “A Power Converter for Photovoltaic Applications”, licentiate thesis, Department of Electric Power Engineering, Chalmers University of Technology, Göteborg, Sweden 2000.

[9] L. Stamenic, G. W. Ingham “A Power for the World - Solar Photovoltaics Revolution”. A Canadian Handbook for electricians, engineers, architects, inspectors and builders.

[10] D. A. Neamen "Semiconductor Physics and Devices", Publisher Irwin 1992

9. Appendices

Appendix A: Measurements from the five inverters

In order to verify the developed inverter system some measurements were made. An ordinary PC was used together with a data acquisition card and DaisyLab software package. During some weeks in the summer 2001, this system was connected to the Sankt Jörgen site.

Verification of the system

In Figure 25 the ac-power from each of the five inverters are shown during a sunny day (2001-07-24).

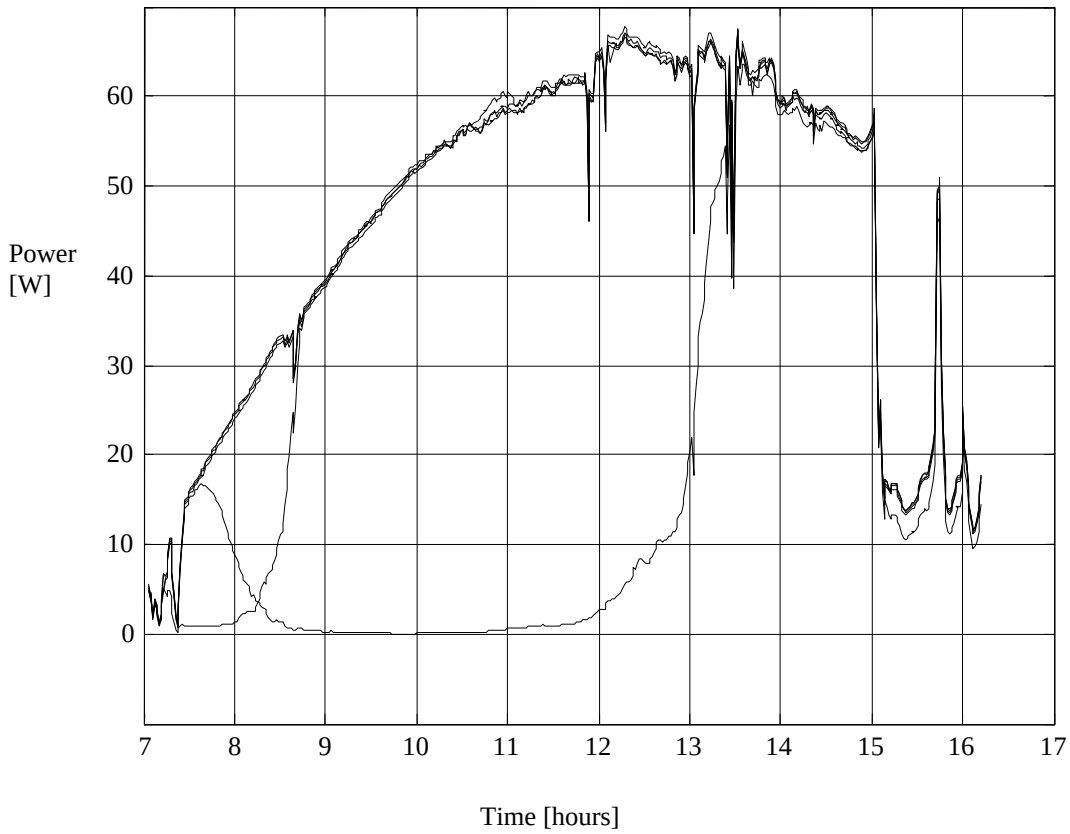

Figure 25, Power from five 110 W inverters.

Three of the inverters are producing approximately the same amount of power while two of the modules are shaded successively. At 8.30 a.m. a shadow from a fan-case moves from the second module to the first and at 1.00 p.m. the shadow leaves that module too. This is how we intuitively

would expect the function of a solar array (and it *is* the case for thermal solar panels). For a conventional string-inverter the total production from these five PV-modules had been substantially lower.

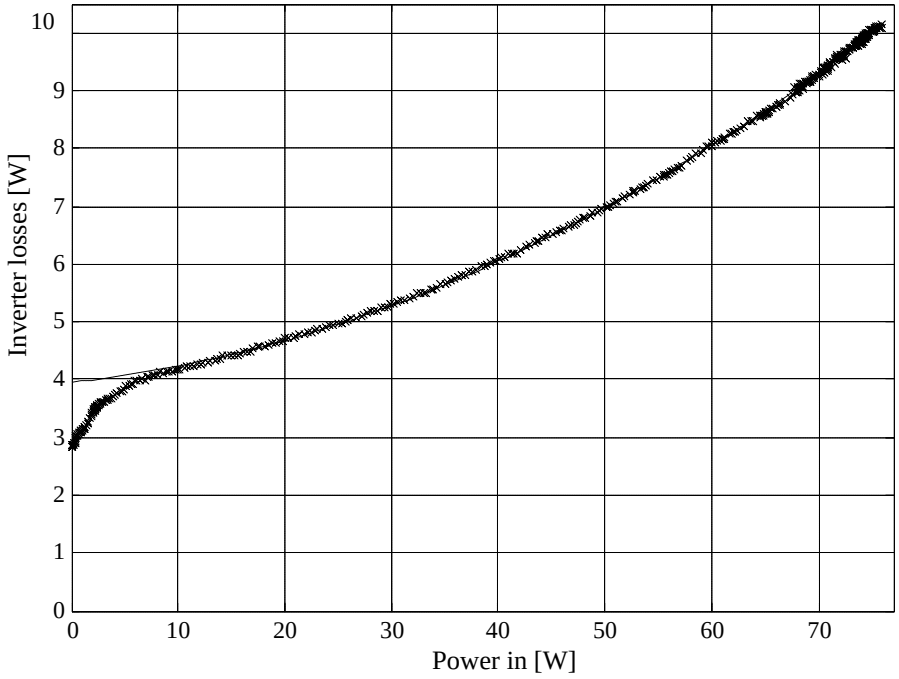

Figure 26, Total losses of one 110 W inverter.

In Figure 26 the power loss in one inverter is shown as a function of power from the PV-module. The controller power supply can be presumed to be approximately 3 W, another 1 W is required when the inverter starts to switch (drivers' supply). Conducting- and iron-losses make the total losses increase approximately quadratic with the power (grid current).

Harmonics

The sampling frequency for the acquisition system used (eight channels) was 4 096 Hz which is high enough to capture the low harmonics but not the switching frequency of 4-8 kHz. (According to the Nyqvist theorem, harmonics up to 2 kHz, or the 40th order can be measured.)

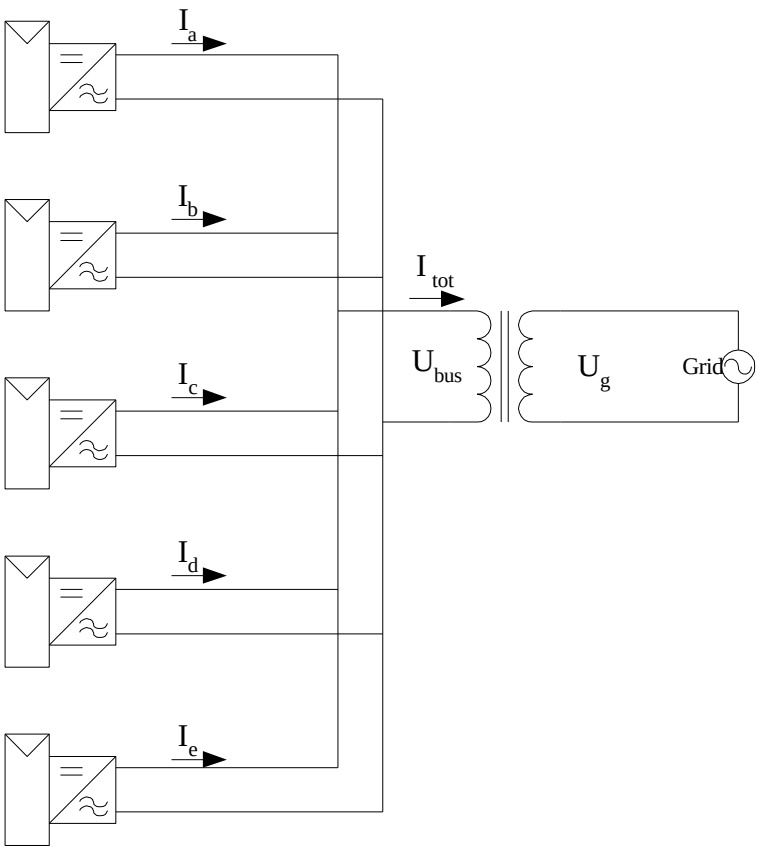

Figure 27, Testsystem at Sankt Jörgen.

The definition of currents and voltages in the system is seen in Figure 27. All are measured but I_{tot}, which is calculated as $I_a+I_b+I_c+I_d+I_e$.

Measurements Table Iare from Sankt Jörgens Park, 2001-07-05 13:45. In Table II the same figures are given normalised to their fundamental frequency, respectively.

Table I Measurements in Amperes.

[A]	Ia	Ib	Ic	Id	Ie	I_tot
I_rms	4.991	4.964	4.925	4.967	4.657	24.430
I_dc	0.248	0.078	0.256	0.137	-0.024	0.694
I_1	4.964	4.947	4.899	4.941	4.640	24.390
I_2	0.030	0.031	0.032	0.037	0.028	0.158
I_3	0.022	0.024	0.016	0.022	0.054	0.137
I_4	0.009	0.009	0.009	0.010	0.009	0.046
I_5	0.080	0.071	0.071	0.079	0.077	0.377
I_6	0.010	0.011	0.012	0.011	0.013	0.057
I_7	0.091	0.080	0.079	0.088	0.079	0.417
I_8	0.005	0.007	0.007	0.006	0.011	0.036
I_9	0.044	0.040	0.039	0.043	0.036	0.203
I_10	0.002	0.003	0.002	0.004	0.004	0.015
I_11	0.006	0.002	0.002	0.008	0.004	0.021
I_12	0.003	0.002	0.002	0.001	0.001	0.004
I_13	0.031	0.022	0.021	0.026	0.030	0.129

Table II Measurements relative fundamental harmonic.

	Ia	Ib	Ic	Id	Ie	I_tot
I_dc	5.0%	1.6%	5.2%	2.8%	-0.5%	2.8%
I_1	100.0%	100.0%	100.0%	100.0%	100.0%	100.0%
I_2	0.6%	0.6%	0.7%	0.7%	0.6%	0.6%
I_3	0.4%	0.5%	0.3%	0.4%	1.2%	0.6%
I_4	0.2%	0.2%	0.2%	0.2%	0.2%	0.2%
I_5	1.6%	1.4%	1.4%	1.6%	1.7%	1.5%
I_6	0.2%	0.2%	0.2%	0.2%	0.3%	0.2%
I_7	1.8%	1.6%	1.6%	1.8%	1.7%	1.7%
I_8	0.1%	0.1%	0.1%	0.1%	0.2%	0.1%
I_9	0.9%	0.8%	0.8%	0.9%	0.8%	0.8%
I_10	0.0%	0.1%	0.0%	0.1%	0.1%	0.1%
I_11	0.1%	0.0%	0.1%	0.2%	0.1%	0.1%
I_12	0.1%	0.0%	0.0%	0.0%	0.0%	0.0%
I_13	0.6%	0.4%	0.4%	0.5%	0.6%	0.5%

The dc-components in I_a and I_c seem to be high. It is possibly a calibration error, not a real value. Unfortunately the measurement equipment was removed before this was discovered and the matter could not be investigated. Harmonic component 5 and 7 are dominating and this is also noted for simulations in Paper G.

In Table III harmonic distortions are given as: total, low frequency even, low frequency odd and high frequency (> 13th) distortions.

Table III THD in Amperes and relative fundamental harmonic.

	Ia	Ib	Ic	Id	Ie	I_tot
THD	0.517	0.416	0.514	0.509	0.398	1.391
relative	10%	8%	10%	10%	9%	6%
THD_lf_e	0.034	0.035	0.037	0.040	0.034	0.179
relative	0.7%	0.7%	0.7%	0.8%	0.7%	0.7%
THD_lf_o	0.135	0.119	0.116	0.130	0.132	0.627
relative	2.7%	2.4%	2.4%	2.6%	2.8%	2.6%
THD_hf	0.431	0.390	0.429	0.470	0.373	1.013
relative	8.6%	7.8%	8.7%	9.5%	8.0%	4.1%

The even harmonics are lower than the odd harmonics. The conclusion from Paper G that the high frequencies are relatively lower when added seems to hold. Table IV gives the relative harmonic components of the voltages. The third and ninth harmonics are dominating but they do probably originate from other devices on the grid.

Table IV Harmonics on the voltage relative fundamental.

	U_bus	**U_grid**
U_dc	-0.20%	-0.33%
U_1	100.00%	100.00%
U_2	0.07%	0.02%
U_3	0.58%	0.60%
U_4	0.03%	0.01%
U_5	0.28%	0.27%
U_6	0.01%	0.01%
U_7	0.22%	0.18%
U_8	0.02%	0.01%
U_9	0.38%	0.36%
U_10	0.01%	0.01%
U_11	0.19%	0.18%
U_12	0.00%	0.00%
U_13	0.15%	0.17%

Appendix B: Matlab-code for PVSF

```
%calc4.m: Calculates the table for a predefined variable switch frequency with
% a constant ripple (ddi=0) or sinusoidal varying ripple (ddi ~= 0 && ddi < di)
%2000-04-23

t=[];
%Different points of operation on the dc-side
points=[
%[V] & [A]
25 0
45 0
25 3.5
34 3.2
31 2.0
];
if exist('J') ~= 1,
  J=4;  %4=the maximum power point (PV)
end
if exist('di') ~= 1,
  di=1;  %The pre-defined maximum ripple
end
if exist('ddi') ~= 1,
  ddi=0.0; %the amplitude-varyation of the ripple
end
if exist('U_g') ~= 1,
  U_g=15; %Grid voltage
end
if exist('L') ~= 1,
  L=0.001 ; %Grid inductance
end
if exist('t1') ~= 1,
  t1=2e-3; %value in table where output voltages are changed
end
if exist('t2') ~= 1,
  t2=7.5e-3; %value in table where output voltages are changed
end
if exist('f_osc') ~= 1,
  f_osc=10e6; %CPU frequency / the resolution of the table
end

w=314.159265;

U_pv=points(J,1);  %Select a point of operation
I_pv=points(J,2);
P=U_pv*I_pv;
I_g=P/U_g; %If efficiency is 100 %

time=[];
D=[];
T_period=[];
i_g=[];
i_old=0;
i_rip=[];
t_2=[];
t=0;
while t < 10e-3,
  T_max=1e-3;
```

```
  T_min=1/f_osc;
  T_try=50e-6;
  while (T_max-T_min) > 1/f_osc,
    di_period = sqrt(2)*I_g*(sin(w*(t+T_try))-sin(w*t));
    u_Lp=U_pv-sqrt(2)*U_g*sin(w*t);
    if t > t1 & t < t2
      u_Lm = -sqrt(2)*U_g*sin(w*t);
    else
      u_Lm = -U_pv-sqrt(2)*U_g*sin(w*t);
    end
    D_try = (di_period*L/T_try-u_Lm)/(u_Lp-u_Lm);
    di_p=u_Lp/L*D_try*T_try;
    di_m=u_Lm/L*(1-D_try)*T_try;
    if max(abs(di_p),abs(di_m)) > di - ddi*cos(2*w*t)
      T_max=T_try;
    else
      T_min=T_try;
    end
    T_try = 10^((log10(T_max)+log10(T_min))/2); %new value of T_try
  end
  i_rip=[i_rip;i_old+di_p; i_old+di_period];
  i_old=i_old+di_period;
  t_2=[t_2; t+D_try*T_try];
  T_period = [T_period; T_try*f_osc];
  t = t + T_try;
  t_2=[t_2; t];
  time=[time; t];
  D=[D; D_try];
  i_g=[i_g; sqrt(2)*I_g*sin(w*t)];
end

f_min=1e7/max(T_period)
f_av = max(size(time))*100
f_max = 1e7/min(T_period)

figure(1)
subplot(111)
plot(t_2,i_rip)
title('i_r_i_p')
grid on

figure(2)
plot(time,[T_period D.*T_period])
title('T period and T_o_n')
axis([0 0.01 0 max(T_period+20)])
grid on

t=(1:98)'/98*0.01;
zone=zeros(size(t));
for I=1:98,
   if t(I) > t1 & t(I) < t2
      zone(I)=1;
   end
end

figure(3)
T=round(interp1(time, T_period, t));
plot([T zone*100],'x')
title('T')
grid on
```

Paper A:

P. Carlsson and L. Cider, B. Lindgren

Yield Losses due to Shading in a Building-integrated PV Installation; Evaluation, Simulation and Suggestions for Improvements.

Published at the 2nd World Conference and Exhibition on Photovoltaic Solar Energy Conversion, Vienna 1998.

Paper B:

Björn Lindgren

Topology for Decentralised Solar Energy Inverters with a Low Voltage AC-Bus.

Published at the 8th European Conference on Power Electronics an Applications (EPE'99), Lausanne, Switzerland, 7-9 September 1999

Paper C:

Björn Lindgren

A PV-module Oriented Inverter, Feeding a Low Voltage AC Bus.

Published at the 16th European European Photovoltaic Solar Energy Conference and Exhibition, Glasgow, May 2000

Paper D:

Björn Lindgren

A 110 W Inverter for Photovoltaic Applications.

Published in International Journal of
Renewable Energy Engineering, April 2002

Paper E:

B. Lindgren, M. H. J. Bollen, O. Carlson

Implementation of Predefined Variable Switching Frequency in a Grid-connected Inverter for Photovoltaics.

Submitted to IEEE Power Engineering Letters

Paper F:

B. Lindgren, M. H. J. Bollen, O. Carlson

Voltage Control of Low-voltage Feeders with Photovoltaic Generators.

Submitted to IEEE Transactions on Power Delivery.

Paper G:

B. Lindgren, M. H. J. Bollen, O. Carlson

Harmonics on the Grid from Single-phase Hysteresis Controlled Inverters.

Submitted to IEEE Transactions on Energy Conversion.

Paper H:

M. H. J. Bollen, B. Lindgren, O. Carlson

Voltage Drop Along a Feeder with a Large Number of Inverters Equipped with Voltage Control.

Submitted to IEEE Transactions on Energy Conversion.